

# FLUID COMPOSITION ANALYSIS BY MULTIPLE GAMMA-RAY BEAM AND MODALITY MEASUREMENTS

Geir Anton Johansen<sup>1,3</sup> and Stein-Arild Tjugum<sup>2,3</sup>

<sup>1</sup> University of Bergen, Department of Physics and Technology  
Allégaten 55, N-5007 Bergen, Norway  
[geir.johansen@ift.uib.no](mailto:geir.johansen@ift.uib.no)

<sup>2</sup> Roxar Flow Measurement  
PO Box 2364 Solheimsviken, N-5824 Bergen, Norway  
[stein-arild.tjugum@roxar.com](mailto:stein-arild.tjugum@roxar.com)

<sup>3</sup> The Michelsen Centre for Industrial Measurement Science and Technology  
P.O.Box 6031, N-5892 Bergen, Norway

## ABSTRACT

The feasibility of using multiple gamma-ray beams to identify the type of flow regime has been demonstrated. One gamma-source with principal emission at 60 keV is used because this relatively low energy enables efficient collimation and thereby shaping of the beams, as well as compact detectors. One detector is placed diametrically opposite the source whereas the second and eventually the third are positioned to the sides so that these beams are close to the pipe wall. The principle is then straight forward to compare the measured intensities of these detectors through that identify the instantaneous cross sectional gas-liquid distribution. By counting the intensity short time slots and (< 100 ms), rapid regime variations are revealed.

Varying water salinity is another challenge for most multiphase flow meters because it affects volume fraction calculations based on gamma-ray, electrical conductance and other measurements. There have been a few approaches to solve this without relaying on off line calibration. One of these utilizes the difference in the composition of the gamma-ray attenuation coefficient at different energies. The method presented here take advantage of the same effect, but through simultaneous measurements of transmitted and scattered gamma-rays from a <sup>241</sup>-Am source. It has been shown that the gas volume fraction then can be determined independent of changes in the water salinity. Once again the challenge is to minimize the effects of changes in the flow regime.

## 1. INTRODUCTION

Measurement of multiphase pipe flow of gas, oil and water is not at all trivial and in spite of considerable achievements over the past two decades, important challenges remain 1. These are related to reducing measurement uncertainties arising from variations in the flow regime, improving long term stability and developing new means for calibration, adjustment and verification of the multiphase flow meters. This work focuses on the first two issues using gamma-ray attenuation and scattering methods.

Multiphase flow meters operate by combining instantaneous velocity and cross sectional fraction measurements of the flow components. The major source of flow regime induced errors is temporal variations in the distribution of gas and liquid in the measurement cross section of the pipe. The oil/ water distribution is less critical because these components are closer in density - which also implies that they are less likely to be separated. Although flow velocity measurements in some cases may be somewhat affected by temporal variations in the gas/ liquid distribution, the major problem is the component volume fraction measurement principles. Not surprisingly, measurements of the gas volume fraction (GVF) are most susceptible; however, significant errors may also be present in some measurements of the water in liquid ratio (WLR- also known as water cut). This is because the sensitivity of single global measurements is inhomogeneous over the pipe cross section. In this work we attempt to reduce these errors by identifying temporal variations in the flow regime and making the necessary corrections. Gamma-ray attenuation is the most frequently applied principle for GVF measurements and was therefore obvious to investigate the use of multiple gamma-ray beams (MGB). The feasibility of this approach has been proven 2.

Varying water salinity is another challenge for most multiphase flow meters because it affects volume fraction calculations based on gamma-ray attenuation, electrical conductance and other measurements. One approach to solve this without relying on off line calibration utilizes the difference in the composition of the gamma-ray attenuation coefficient at different energies 3. The dual modality method (DMD) method in this work take advantage of the same effect, but though measuring the scatter response with a separate detector in addition to the total attenuation by traditional transmission measurement. It has been shown that the gas volume fraction then can be determined independent of changes in the water salinity [4]. Once again the challenge is to minimize the effects of changes in the flow regime, particularly of the scatter measurements.

## **2. THE DMD AND MBG PRINCIPLES**

### **2.1 Choice of Radioisotope**

The most frequently used radioisotope for GVF measurements in pipe flows is  $^{137}\text{Cs}$  with 662 keV gamma-ray emission. It has a relatively long half life (30 years) and a pure emission spectrum with sufficiently high energy to enable clamp-on installation on pipes. The latter is less important for multiphase flow meters which need to be installed in-line anyway. For successful implementation of the MGB and DMD principles it is a requirement to use an isotope with lower emission energy for several reasons:

- The DMD principle requires sufficiently low energy for photoelectric absorption to make a significant contribution to the total attenuation in the fluid in addition to Compton scatter, see Figure 1. This will be further explained in the next section.
- The MBG principle depends on efficient beam collimation and this can be achieved with much less material (thickness) at low energies.
- It is possible to use smaller and more compact detectors which in combination with less collimation and shielding thickness make it possible to embed both source and detectors in the pipe wall in the final design.

Lower radiation energy also has the advantage of far less radiation dose to the environment 5. The first of these conditions suggest that a gamma-ray energy of about 50 keV would be ideal. Energies lower than this would put severe restrictions on the material, wall thickness and diameter of the pipe. Based on these considerations and the available radioisotopes,  $^{241}\text{Am}$  was selected as source. For all practical purposes this has a pure emission spectrum with principal energy at 59.5 keV and also a long half-life (432 years).

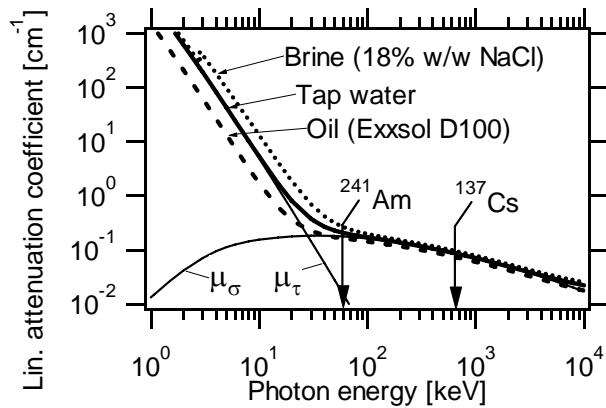


**Figure 1.** The linear gamma-ray attenuation coefficient of oil, water and brine as a function of energy. Its contributions from Compton scattering ( $\mu_{\sigma}$ ) and photoelectric absorption ( $\mu_{\tau}$ ) are shown for tap water. The emission lines of  $^{241}\text{Am}$  (60 keV) and  $^{137}\text{Cs}$  (662 keV) are also shown.

## 2.2 Dual Modality Densitometry for Salinity Measurements

The foundation of the dual modality principle is that Compton scattering is roughly proportional to the density of the fluid ( $\mu_{\sigma} \sim \rho$ ), whereas the photoelectric absorption coefficient is strongly dependent on its atomic composition ( $\mu_{\tau} \sim Z^4$  to  $Z^5$ ) 5. This makes the latter very sensitive to salt elements such as chlorine because of their higher atomic numbers (Z). To enable measurements of these two components, two detectors are used as illustrated in Figure 2.

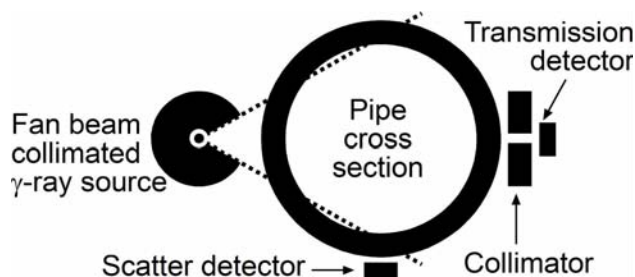


**Figure 2.** The DMD measurement geometry using one transmission detector and one scatter detector 4.

The total attenuation measured by the transmission detector will have contributions from both photoelectric absorption and Compton scatter. The response is expressed by Lambert-Beer's exponential decay law provided a fairly strict detector collimation is applied to avoid forward

scatter contribution (build-up). The scatter detector is positioned outside the direct view from the source and will thus not detect any directly transmitted radiation at all. Its response will solely be measurement of radiation originating from Compton scatter in the pipe cross section. The transmission detector thus provides a measurement of both the photoelectric and Compton scatter coefficients, whereas the scatter detector mainly provides a measurement of the Compton coefficient. The response in the latter will also have a small contribution from photoelectric absorption through the attenuation of scattered radiation between the measurement cross section and the scatter detector.

Several semi-empirical models have been developed for the response in the scatter detector 6. They all use the proportionality of the scatter response to the number of scatter events generated over the pipe diameter ( $d$ ) or active volume:

$$I_s \sim \frac{\mu_\sigma}{\mu} [1 - \exp(-\mu(1 - GVF)d)] \quad (1)$$

Here  $\mu$  and  $\mu_\sigma$  are the total and Compton linear attenuation coefficients of the fluid, respectively. In addition corrections must be made for attenuation of the incident beam before it reaches the active volume, and for that of the scattered radiation. Since the scatter emission is isotropic and the geometrical factor of the scatter detector is small, it is advantageous to have Compton dominant attenuation in the fluid, but yet some contribution from photoelectric absorption to monitor the salinity. As can be seen from Figure 1, this is fulfilled at 60 keV.

Accurate semi-empirical models of the scatter response are just the first step in calculating the water salinity in addition to the  $GVF$ . It turns out that that it is more efficient to correct for changes in the water salinity directly by using a simple empirical relationship between the measured transmitted ( $I_T$ ) and scattered ( $I_S$ ) intensities:

$$R = \frac{I_S}{I_T^n} \quad (2)$$

Several experiments with different geometries confirm that this ratio varies with the  $GVF$ , but not with the water salinity. In other words it provides salinity independent  $GVF$  calculation. The exponent is in most cases  $n \approx 0.55$ , but is slightly dependent on the measurement geometry. Its value is found from calibration measurements. The results of the first pilot project, which was carried out with static fluid at controlled conditions, are shown in Figure 3. A limited number of experiments with oil (Exxsol D100) indicate that the slope of the calibration curve varies with the WLR (water liquid ratio). So, as otherwise in calculation of the flow parameters in multiphase flow metering, iterative methods must be applied to solve the set of transcendental equations. These, and later results call for more extensive experiments with a larger variety  $GVF$  and  $WLR$  combinations at different salinity. Another issue also revealed in the pilot project is that the salinity independence of the empirical expression in Equation 2 fails for annular type of flow regimes. So this is yet another example on a multiphase measurement principle that requires knowledge about the flow pattern.

### 2.3 Flow Regime Identification using Multiple Gamma-Ray Beams

Most of today's multiphase flow meters rely on T-bend vertical installation to achieve some degree of fluid homogeneity in the measurement cross section. But even at moderate  $GVF$ s slug flow with annular type of flow pattern is quickly established causing traditional gamma-ray densitometers to overestimate the  $GVF$ . This is compensated for using models taking into account the difference in  $GVF$  inside the beam to that of the full cross section. However, the flow regime depends on a range of factors making it difficult to use general models to correct the  $GVF$ .

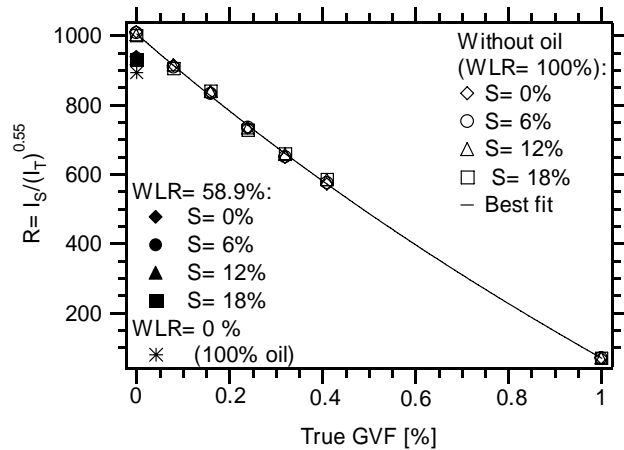


**Figure 3. Calibration curve yielding GVF from measurements of  $I_T$  and  $I_S$  for homogeneously mixed fluid conditions 4. The water salinity (w/w NaCl) percentage is listed with the legends, so is the WLR in the case of  $GVF=0$ .**

An experiment using one fan-beam collimated gamma-source and 9 detectors to cover the full pipe cross section was carried out at the flow loop facility of Christian Michelsen Research 2. The apparatus, which is shown on the top in Figure 4, was mounted in a tilt section and several measurement series were performed with horizontal, 45° tilted and vertical flows. The results for a typical series are shown in Figure 4. The counting or integration time of the 9 detectors are 30 ms, meaning each of the 3 s long sequences presented are composed of 100 individual measurements. All three cases are typical slug flow regimes where it is difficult to measure the  $GVF$  accurately using one beam densitometer and model compensation. But by dividing the flow into short segments as presented in Figure 4, it is possible to continuously identify the instant cross sectional flow pattern. For the horizontal case it can be seen that this typically varies between what would be stratified and bubble type of regime if it was continuous. Likewise the vertical case is composed of bubble and annular flow. For the tilted flow case a mixture of all patterns can be identified although it can be most closely associated with horizontal flow. This is probably because the measurement position is just about 2 m above the floor level where the flow enters the tilt section. It would look different if the tilted flow was allowed to develop further. In all cases the limited spatial measurement resolution makes bubble flow, which is typical for low gas fractions, appear as homogeneously mixed flow for the detectors.

The conclusion of this work was that it is possible to use multiple gamma-ray beams to continuously identify the instantaneous flow pattern in multiphase pipe flow. This can in turn

be used to calculate the GVF more accurately and also to correct other measurements, such as the DMD GVF, according to their dependency.

A practical implementation of the MGB principle needs to be simpler and more compact than the system shown in Figure 4. A system with the source and detectors partially embedded in the pipe wall has been built and successfully tested <sup>7</sup>. This uses only two transmission detectors to identify the regime. A similar set-up is presented in the next section.

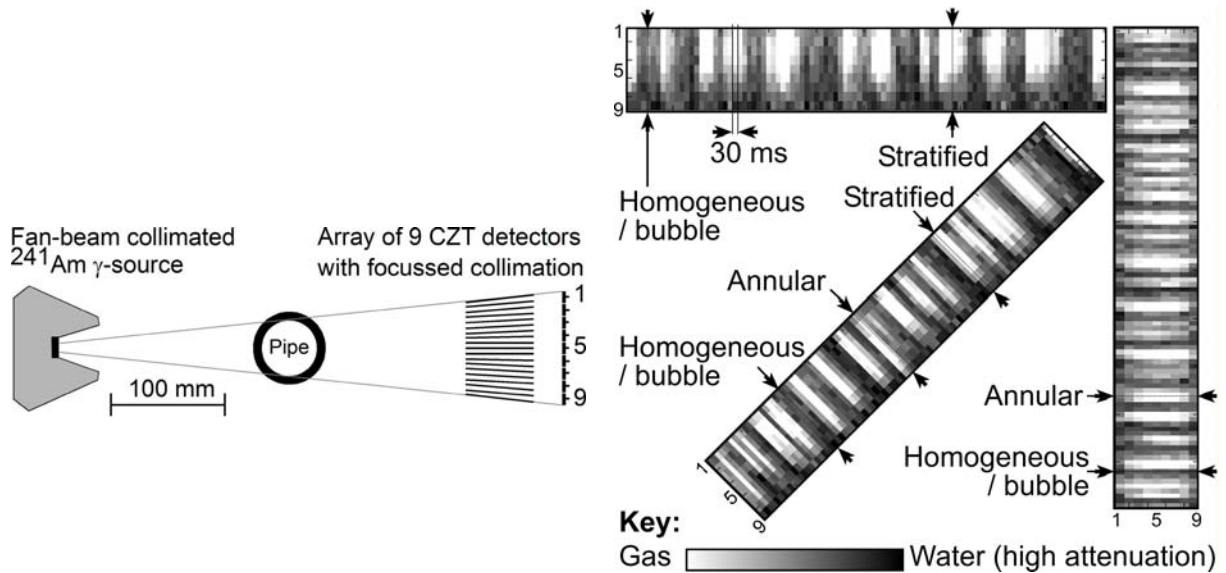


**Figure 4. Experimental set-up (top) and measured three phase flow pattern sequences with  $Q_{oil}=5 \text{ m}^3/\text{h}$ ,  $Q_{water}=25 \text{ m}^3/\text{h}$  and  $Q_{gas}=20 \text{ Am}^3/\text{h}$  (83% WLR and 67% GVF) average reference data at horizontal, 45° tilted and vertical flow. Each of the 3 s long sequences is composed of 100 separate measurements with 3 ms counting (integration) time. The numbers refer to the array of 1 cm<sup>2</sup> detectors shown at the set-up on the top.**

## 2.4 Experimental Set-up for Rig Tests

To further investigate the DMD and MGB principles an experiment was carried out using a basic circulation flow loop rig which uses Diesel oil, saline water and compressed air as gas. The WLR is set by filling the bottom tank, which also is the gas/ liquid separator, with the desired amount of oil and water before each run. Compressed air is injected continuously under the runs through a separate valve. The actual salinity and WLR for each run are determined by sampling the fluid at a point with fairly homogeneous mixing. An YSI Model 30M/10FT probe is used for salinity measurement, whereas the WLR is determined by fractional measurements of the liquid sample after separation. Compared to a large flow loop facility where the oil and water are continuously separated in a large volume tank, the limited volume of this system makes it fairly easy to change the water salinity (using NaCl) before each run. For all runs the flow is allowed to stabilize before the data acquisition is started.

The measurement geometry for the experiments is shown in Figure 5 and based on the conclusions of previous work as presented in sections 2.2 and 2.3. A PVC spool piece with 81 mm diameter was used in the measurement cross section. This has approximately the same

attenuation properties as PEEK or reinforced epoxy which typically are used in a real flow meter system. All four detectors are CsI(Na) scintillation counters with integrated read-out electronics and counter output. The size of the crystals is  $\varnothing = 13 \text{ mm} \times 38 \text{ mm}$ . Both DMD scatter detectors (S1 and S2) have fairly relaxed collimation to allow higher count-rate and make it comparable with that of the transmission detectors. The transmission detectors (T1 and T2) are collimated to reduce build-up for the DMD measurements, and to reduce their fields of view for the flow pattern identification. The experiments were to a large extent carried out by an MSc student 8.

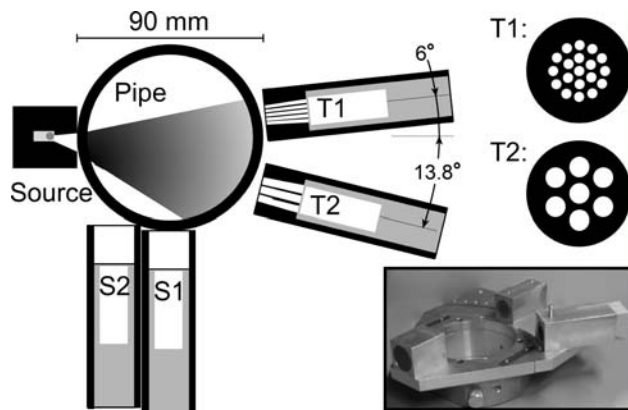


**Figure 5.** The MBG DMD measurement geometry used for the rig experiments. The shaded area in the pipe is the beam as defined by the source collimation. The shading indicates the exponential decay in the number of interactions across the pipe for homogeneously mixed flow. This is highest in the dark area close to the source. The insert show the source and detector support system (without scatter detectors) which is clamped onto the pipe. Also shown are cross sections of the focused collimators used for T1 and T2 with  $\varnothing = 2 \text{ mm}$  and  $\varnothing = 4 \text{ mm}$  holes, respectively.

### 3. RESULTS

In Figure 6 the ratio given in Equation 2 is plotted for all four combinations of scatter and transmission detector intensities. The  $WLR$  is close to 100%, i.e. there is virtually without oil, and three different salinities are used. As can be seen the salinity independent  $GVF$  principle is confirmed for all ratios, however, the  $R_{11}$  ratio clearly provides the highest sensitivity.

In Figure 7  $R_{11}$  is plotted as a function of  $GVF$  for three different salinities and four different  $WLRs$  ranging from 20% to 99%. The results presented in Figure 3 are partially confirmed as the presence of oil in the flow reduces the slope of the calibration curve ( $R$  -vs-  $GVF$ ) as expected. But it also shows that the  $WLR$  need to be known (which it is in multiphase flow meters) to maintain salinity independent  $GVF$  measurements at low  $WLRs$ . In the plot this is most clearly seen for  $WLR = 20\%$  and  $WLR = 25\%$  at  $GVF = 0$ ; these should appear on the same spot, but they do not. The effect of a range of the  $n$ -values (the exponent in Equation 2) was investigated, but did not make a significant change. The same plot was made for  $R_{12}$ ,  $R_{21}$ , and  $R_{22}$ , and for their mean  $R_{AVG}$ , but the results were the all same. The only difference was the slope of the calibration curve, i.e. the sensitivity, as can be seen for  $R_{AVG}$  in Figure 7.

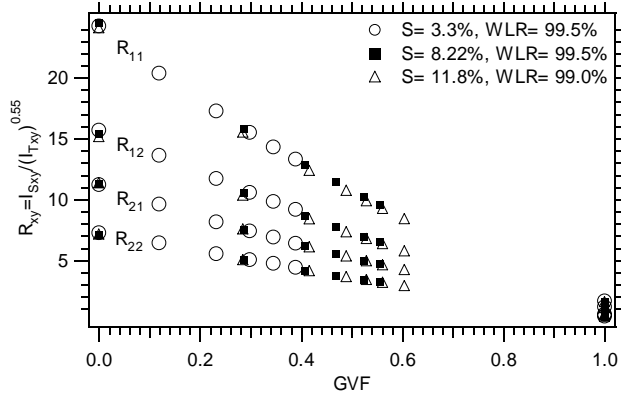


**Figure 6. Plot of the R ratio (Equation 2) -vs- GVF of the four possible combinations of transmission and scatter detectors shown in Figure 5 ( $R_{12} = I_{S1}/(I_{T2})^{0.55}$  etc.) with three different salinities (S) and  $WLR \approx 100\%$ .**

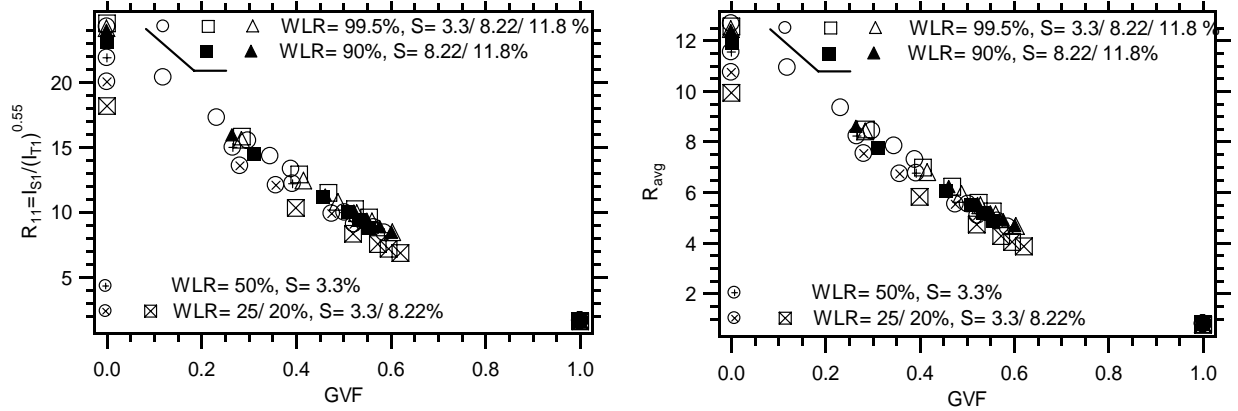


**Figure 7. The ratio  $R_{11}$  (Equation 2) -vs- GVF at three different salinities and four different WLRs (left) and with the average ratio  $R_{AVG} = (R_{11} + R_{12} + R_{21} + R_{22})/4$  (right).**

Previous experiments 4 indicate that annular type of flow would have the same effect on the salinity independence as seen here although it does not explain the deviation of identical WLRs at  $GVF=0$ . Whilst there is no possibility that annular flow has developed fully at the measurement point in the loop, it is likely that there will be slug flow with temporal annular type of pattern as can be seen in the vertical plot in Figure 3. To check for this the GVF was calculated from both T1 ( $GVF1$ ) and T2 ( $GVF2$ ) intensity measurements,  $I_T$  5:

$$GVF \approx \ln \left[ \frac{I_T}{I_W} \right] / \ln \left[ \frac{I_G}{I_W} \right] \quad (3)$$

Here  $I_W$  and  $I_G$  are calibration measurements at  $GVF=0$  and 1, respectively. Since there is no reference data available for the GVF in the flow rig,  $GVF2$  is plotted as a function of  $GVF1$  in Figure 8. The result shows that  $GVF1$  in all cases are higher than  $GVF2$ . To see how this relationship would be with an exact GVF reference and a true annular flow pattern, a MCNP5 Monte Carlo model was developed for the system and benchmarked at  $GVF=0$  and 1, and at  $WLR=0$  and 100% for all detectors. A cylinder shaped gas bubble was introduced along the

center axis of the pipe and simulations were made with stepwise increases in the radius of this cylinder. The results are also plotted in Figure 8 where  $GVF1$  and  $GVF2$  and their errors are shown as functions of the true  $GVF$  determined by the ratio of the cylinder. Simulations of homogeneously mixed flow end up on the straight line as one would expect.

#### 4. DISCUSSION

The measured results presented in Figure 8 predict that there is a predominant distribution of gas along the center axis of the pipe for all measurements. This is confirmed by the simulations. The deviation between the measurements and the simulations at low  $GVF$ s is explained by the fact that it is unlikely to have a stable gas core at the pipe center at these conditions. The simulation results presented in Figure 8 confirm that there, except for high gas fractions, always is a difference between  $GVF1$  and  $GVF2$  with this geometry.

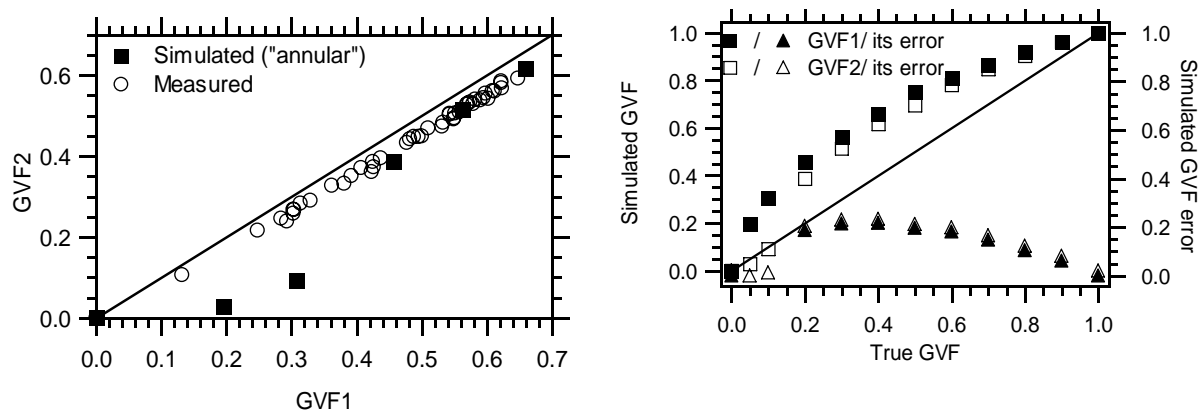


**Figure 8. Calculated  $GVF2$  plotted versus calculated  $GVF1$  for all measured data sets and for simulations on annular type flow with 3.3% brine (left), and calculated  $GVF1$  and  $GVF2$  and their errors based on simulations plotted as functions of the true  $GVF$  with 3.3% brine as liquid phase (right).**

This means that the actual  $GVF$  is less than that presented in Figs. 6, 7 and 8. This adds uncertainty to the quality of the data presented in these figures. Further Monte Carlo simulations would be helpful here since these provide accurate reference data.

Regarding positioning of the scatter detectors the results confirm that S1 is an ideal position because it has higher sensitivity than S2 to the full pipe cross section. The less favorable result with S2 may be explained by its higher contribution from the pipe wall and partly source collimator, and correspondingly less from the fluid. Better results would probably be achieved with S2 if it were tilted slightly towards the center of the pipe.

#### 5. CONCLUSIONS

The lack of accurate reference data for the measurements makes it difficult to make solid conclusions. Nevertheless the support of Monte Carlo simulations confirms that the applied measurement geometry can be used to identify the average flow pattern and correct for  $GVF$

errors. However, the sensitivity to annular type of flow pattern would be higher with detector T2 placed at a higher angle, such as 25° or slightly more.

The results also show that the DMD principle for salinity correction has highest sensitivity with the scatter detector positioned as S1 with a large field of view. On the other hand the results indicate that the DMD salinity compensation fail at low WLR, but this is uncertain because of lack of accurate reference data.

Further research should be carried out with Monte Carlo simulations since this provides accurate reference data which experimentally is very difficult to achieve in any flow loop. A major advantage in both the DMD and MBG principles is that they rely on pulse counting only; there is no need for detectors with high energy resolution and read-out electronics to perform energy analysis.

## ACKNOWLEDGEMENTS

The support on Monte Carlo simulation by Prof. Robin P. Gardner and the CEAR members at North Carolina State University is very much appreciated.

## REFERENCES

1. S. Corneliussen, J.-P. Couput, E. Dahl, E. Dykesteen, K.-E. Frøysa, E. Malde, H. Moestue, P.O. Moksnes, L. Scheers and H. Tunheim *Handbook of Multiphase Flow Metering*, Rev. 2, 2005 ([www.nfogm.no](http://www.nfogm.no)) NFOGM/ Tekna.
2. S.-A. Tjugum, B. T. Hjertaker and G. A. Johansen “Multiphase flow regime identification by multibeam gamma-ray densitometry” *Meas. Sci. & Technol.* 2002, **13**, 1319-1326.
3. A. M. Scheers, “Multiple Energy Gamma Ray Absorption (MEGRA) Techniques Applied to Multiphase Flow Metering”, 1998, *Proceedings of the 4th Int. Conf. on Multiphase Techniques*, London 26 & 27 March.
4. G. A. Johansen and P. Jackson “Salinity independent measurement of gas volume fraction in oil/gas/water pipe flows”, 2000, *Appl. Rad. and Isotopes* **53** No. 4-5, 595-601.
5. G. A. Johansen and P. Jackson *Radioisotope gauges for industrial process measurements* John Wiley & Sons, Ltd. (2004) 336 pp.
6. S.-A. Tjugum, G. A. Johansen and J. Frieling “A multiple voxel model for scattered gamma radiation in pipe flow” *Meas. Sci. & Technol.* **14** No 10 (2003) 1777-1782.
7. S.-A. Tjugum, J. Frieling and G. A. Johansen “A compact low-energy multibeam gamma-ray densitometer for pipe-flow measurements” *Nucl. Instr. & Meth.* **B197** (2002) 301-309.
8. L. Ratnam *DMD experiments in a three phase flow loop* (in Norwegian) MSc thesis at the Department of Physics and Technology, University of Bergen (2006).